INSTITUTE OF PLASMA PHYSICS
CZECHOSLOVAK ACADEMY OF SCIENCES

QUASI - OPTICAL GRILL MOUNTED IN HYPERGUIDE

J. Preinhaelter

RESEARCH REPORT

IPPCZ - 348 April 1995

POD VODÁRENSKOU VĚŽÍ 4, 180 69 PRAGUE 8
CZECHOSLOVAKIA

QUASI-OPTICAL GRILL MOUNTED IN HYPERGUIDE

J. PREINHAELTER

IPPCZ-348 April 1995

QUASI-OPTICAL GRILL MOUNTED IN HYPERGUIDE

J. PREINHAELTER

Institute of Plasma Physics
Czech Academy of Sciences
Za Slovankou 3, P.O.B. 17
182 11 Praha 8
Czech Republic

ABSTRACT

Proposal of a new launcher of the lower hybrid waves for the current drive in future big thermonuclear facilities operating at 10 GHz frequency range is given. We combine the principle of the quasi-optical grill with the concepts of the hyperguide and the multijunction grill. As an example we optimize a six rod structure mounted in a oversized waveguide and irradiated by the oblique plane wave emerging in the form of a higher mode from an auxiliary oversized waveguide. The rods of the optimum structure have the elongated form of the cross-section with the resonant length (in the direction of wave propagation) equal to a multiple of half wavelength of the fundamental mode of hyperguide. This row of rods forms a multijunction grill with the zero phase shift between waveguides. The second row of rods supporting the constructive superposition of the incident and doubly reflected waves enhances the efficiency of the structure. The optimum structure has the power spectrum with two narrow peaks (the main $N_{\parallel} = -2.15$ and the parasitic $N_{\parallel} = 3.15$), the low power reflection ($R_{tot} = 15\%$), the high coupled power directivity ($\delta_{CP} = 70\%$), the reasonable $N_{\parallel}$-weighted directivity ($|\delta^{w}_{CD}| = 35\%$) and the peaking factor on the electric field equal to 3. On the basis of the optimization it is possible to design the parameters of a big structure with tens of rods. The number of the construction elements of this structure can be reduced 20-times in comparison with the standard multijunction array.

1 Introduction

It is generally accepted that the lower hybrid current drive and the plasma heating should play an important role in the modern large thermonuclear facilities. Because the magnetic field intensity is here greater than 5 T, the frequency of the lower hybrid waves used for the current drive can reach 10 GHz. Thus the development of an alternative wave launcher is urgent. The waveguides of the contemporary multijunction grill would have to be very narrow with the thin walls between them. Cooling of such structure is very difficult and influences design of the present launchers strongly (eg the "passive-active" structure operating at 3.7 GHz on TORE SUPRA or the similar structure for ITER [1]). The quasi-optical launcher of the lower hybrid waves, which was originally presented as an infinite set of circular rods placed in a free space in front of a plasma and irradiated obliquely by the properly polarized plane wave, offers one possible solution of this problem [2].

To make clear the preceding statement we compare the periodicity length $z_{\mathrm{MJG}}^{\mathrm{period}}$ of the standard multijunction grill (the width of one waveguide plus the thickness of the wall separating the individual waveguides) with the same quantity $z_{\mathrm{QOG}}^{\mathrm{period}}$ for the quasi-optical grill (the width of the gap between rods plus the rod diameter). The Floquet's theorem, determining the positions of N_z-peaks in the space power spectrum of waves radiated into a plasma, gives for MJG

$$N_z = \frac{\Delta o}{k_v z_{\mathrm{MJG}}^{\mathrm{period}}} + \frac{2\pi s}{k_v z_{\mathrm{MJG}}^{\mathrm{period}}}, \quad s = 0, \pm 1, \pm 2, \ldots \tag{1}$$

where $\Delta\phi$ is the phase shift between the adjacent waveguides, k_v is the vacuum wavevector equal to ω/c and s determines the diffraction order. If we require that the wavelength λ_z of waves in the plasma along the toroidal magnetic field is a half of the vacuum wavelength λ_v ($N_z = 2$) and if we consider the main peak ($s = 0$) and the current drive phasing ($\Delta o = \frac{\pi}{2}$), we have $z_{\mathrm{MJG}}^{\mathrm{period}} = \frac{\lambda_v}{8}$, what gives 3.7 mm for $f = 10$ GHz.

For the quasi-optical grill we have much more satisfying result. In this case the Floquet's theorem has a form

$$N_z = N_z^{\mathrm{inc}} + \frac{2\pi s}{k_v z_{\mathrm{QOG}}^{\mathrm{period}}}, \quad s = 0, \pm 1, \pm 2, \ldots \tag{2}$$

where $N_z^{\mathrm{inc}} = k_z^{\mathrm{inc}}/k_v = \sin\alpha$, α is the angle of incidence of a vacuum wave incident obliquely on the rods. Here the zero diffraction order does not contribute to the spectrum of waves in a plasma ($| N_z^{\mathrm{inc}} | < 1$) and thus the most important is the order $s = -1$. For $s = -1$, $N_z = -2$ and $\alpha = 30°$ we have $z_{\mathrm{QOG}}^{\mathrm{period}} = \frac{\lambda_v}{N_z^{\mathrm{inc}} + |N_z|} = \frac{\lambda_v}{2.5}$ what gives 12 mm for $\lambda_v = 3$ cm. Thus QOG has three times less construction elements than MJG and instead of three tiny waveguides and walls we have a gap and one huge rod.

The most important reduction in number of the construction elements of QOG follows from the basically unlimited height of rods. To be able to reach the needed phase shift between adjacent waveguides of MJG we must use for the final multijunction section only one mode waveguides, ie they must have the height lower then

λ_v and must be arranged in many rows in the poloidal direction. Thus, for 10 GHz, $N_z = 2$ and $\Delta\phi = \frac{\pi}{2}$, MJG must be assembled from waveguides $\sim 3 \times 25$ mm. The height of the rods of QOG for the same case can be well above 20 cm. The combined saving in the complexity of the construction of QOG in comparison with MJG can reach a factor of more than 20.

A good survey of the present state of the quasi-optical launchers was given at the Workshop on QOG which was held in Prague, April 1994.

The theory of the quasi-optical grill started in 1989 with M. I. Petelin and F. V. Suvorov paper [2]. They considered the infinite number of equally spaced, infinitely long, rods with the circular cross-section placed in one plane parallel to the surface of the homogeneous plasma with the density n higher then the critical density n_{crit}. This array is irradiated obliquely by an electromagnetic wave having the electric field perpendicular to the rods.

M. I. Petelin in Prague presented the new achievements of Russian group of theoreticians [3]. He discussed the effect of the elliptical cross-section of rods, which improves the efficiency of the s=-1 space harmonic generation, if the long axis of ellipse is parallel to the incident ray. He also mentioned that the reflection coefficient of QOG formed by two rows of rods can be practically zero if the distance between rows fulfils resonance condition.

F. Santini, M. Santarsiero and G. Schettini described the diffraction of an electromagnetic wave incident obliquely on N infinite rods of the circular cross-section arranged in one or two rows in a free space in front of a plasma [4]. The main row (at plasma) consists of the "strips" of two cylinders imitating thus the cross-section of rods elongated in one direction. They solved the problem by the full wave method and thus their numerical results are reliable. It seems, that for the finite number of rods ($N = 6, 8, 9$), they were not able to reach, even in the case of two rows, the power reflection coefficient lower than 50%.

The quasi-optical grill with the rods represented by flat strips was described by G. Tonon. The pessimistic conclusions about the efficiency of QOG expelled by J. P. Crenn and P. Bibet in the conclusion of [5] are questionable because in the flat strip model one important parameter, ie the length of rods in the direction of the wave propagation, is missing. Also the method of solution of this diffraction problem - some mixture of the "equivalent circuits" with the far field formula from diffraction of light on a grating - does not seem fully adequate.

All these structures are supposed to be placed in a free space and to be irradiated by a plane wave. The rods are infinitely long and, in some models, the infinite number of rods is assumed. In the experiments all these assumptions are inadequate - the structure is bounded with some confining walls, the number of rods is finite, it is difficult to create a plane wave. The paraboloid mirrors used for the irradiation of rods calls for the "point-like" source and thus all power must come through one narrow waveguide. The waves reflected from the walls distort the spectrum because their angles of incidence are partly unpredictable and partly unsuitable. It is not solved how to annihilate the power reflected from the plasma in the space filled up with the mirrors and the feeding equipment.

All these problems can be solved by a new structure in which the rods are placed

in one oversized waveguide - hyperguide - and irradiated obliquely by the wave emerging in a form of the higher mode from an auxiliary oversized waveguide. The confining walls are now an intrinsic part of the structure, there are no mirrors, no point-like source and the reflected power can be handled by the standard waveguide technic. The structure is compact, it is highly effective and the problem of the the wave diffraction can be easily solved by the full wave method. The first proposal of such a structure was given by the author in [6], where the preliminary numerical results were also presented.

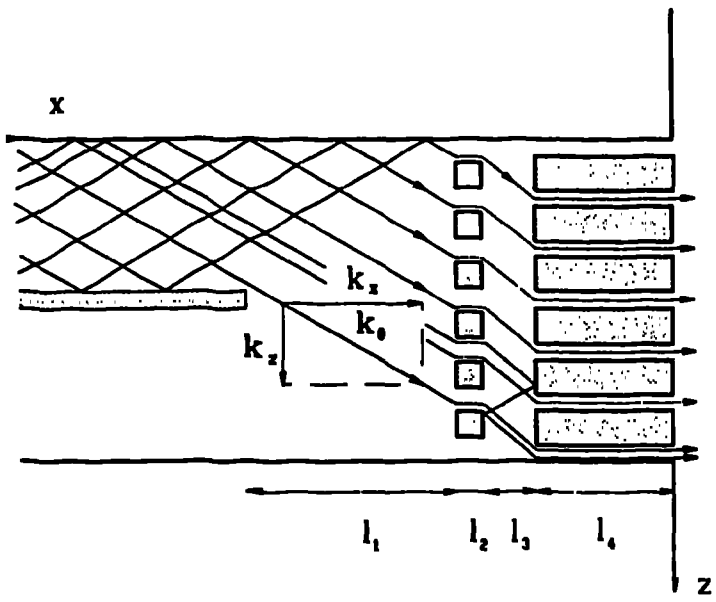

Figure 1: Section through our quasi-optical grill through the plane perpendicular to the rods. Two rows of rods are depicted and the ray trajectories corresponding to the incident higher mode in the auxiliary waveguide are indicated.

In Fig. 1 we see a section of the suggested structure through the plane perpendicular to the rods. The whole structure is mounted in one oversized waveguide, with the rectangular cross-section $a \times b$, whose shorter side b is parallel to the plane of our section and whose axis lies in the plane of the section. In the mouth of this waveguide one or two rows of rods are placed. On the opposite side the main waveguide is split into two oversized rectangular waveguides. In one of them the higher mode is incident having the electric field perpendicular to the rods. The z-component of the electric field of this mode near the axis of the waveguide has a form $E_z \sim \cos(k_z z)e^{ik_x x}$.

To make clear how the structure operates we depicted in Fig. 1 the set of the geometric optics rays corresponding to this mode (we suppose that the height a of the waveguide is much larger then its width so that k_y/k_v is sufficiently small).

If we choose the distance $l_1 + l_3 = (b/2)\cot\alpha$, where the angle of the incidence $\alpha = \arctan(k_z/k_x)$, the rods are obliquely irradiated by the plane wave. The row of rods at the grill mouth forms a multijunction grill with the zero phase shift between the adjacent waveguides. The set of these rods forms an open resonator and the efficiency of the structure is highly improved if the rods are elongated in the direction of the wave propagation so that their length $l_4 = m\lambda_0/2$, where λ_0 is the wavelength of the fundamental mode TE_{10} and m is a natural number. The distance between rows $l_3 = \frac{\lambda_0}{2}\cos\alpha$ ensures that the incident and doubly reflected waves are in phase and thus it improves the overall efficiency of the structure. To simplify mathematics and to obtain an efficient numerical code describing the diffraction of waves in this structure we choose the rods with the rectangular cross-sections. We start the optimization process with thickness of the rods perpendicular to the waveguide axis equal to $\lambda_v/4$ as it was found optimum for QOG in a free space ([3] [4]). Such a structure involves the concepts of the quasi-optical grill, the multijunction grill and the hyperguide in one compact launcher which J.G. Wegrowe envisaged in the closing speech of the Prague Workshop. In the next section we give the outline of the theory describing the diffraction of waves in such a structure. We use for this purpose the theory of the standard multijunction grill developed by the author [7] and we generalize it for hyperguides, rods and an additional waveguide splitting.

In the third section we give the results of the numerical optimization of the launcher having six rods operating at 9.6 GHz. Similar structure but with smaller dimensions is under construction in Prague and it will soon operate at CASTOR tokamak [8].

In the last section the main conclusions are summarized.

2 Theory of the quasi-optical grill mounted in the hyperguide

In Fig. 2 we see the section through the considered structure where all relevant parameters are denoted. The coordinates are chosen so that the x-axis is directed into the plasma (parallel to the density gradient), the z-axis is parallel to the toroidal magnetic field and the y-axis has the poloidal direction. It is supposed the structure has the uniform height a in the y-direction. The whole structure can be divided into five regions. The first one has two subregions, each of them is formed by an oversized waveguide with the rectangular cross-section $a \times b_1$. These two waveguides are separated by a wall with the thickness d_1. The regions $\{2\}$ and $\{4\}$ are the hyperguides $a \times b$. The region $\{3\}$ consists of $N_{rod} + 1$ narrow waveguides $a \times b_3$ separated by N_{rod} rods ($l_2 \times a \times d_3$). This row of rods only slightly enhances the overall efficiency of the structure and can be omitted. The region $\{5\}$ is the most important for the wave diffraction and is formed by the $(N_{rod}+1)$-waveguide multijunction grill with the zero phase shift between individual waveguides. These waveguides have the cross-section $a \times b_5$ and are separated by the huge rods ($l_4 \times a \times d_5$).

Each subregion of our structure can be regarded as a portion of the waveguide with the rectangular cross-section and thus the electric and magnetic fields of the

incident and the reflected waves can be expressed as a sum of modes

$$
\begin{aligned}
E_z^{\alpha,\beta} &= \sin\frac{\pi y}{a}\sum_{n=0}^{\infty}\left(A_n^{\alpha,\beta}\,\mathrm{e}^{ik_n^{\alpha}(x-x_\alpha)} + B_n^{\alpha,\beta}\,\mathrm{e}^{-ik_n^{\alpha}(x-x_\alpha)}\right)\\
&\quad\times\cos\frac{n\pi(z-z_{\alpha,\beta})}{b_\alpha},\\
H_y^{\alpha,\beta} &= \sin\frac{\pi y}{a}\sum_{n=0}^{\infty}\frac{(k_0)^2}{k_{\mathrm{v}}k_n^{\alpha}}\times\left(-A_n^{\alpha,\beta}\,\mathrm{e}^{ik_n^{\alpha}(x-x_\alpha)} + B_n^{\alpha,\beta}\,\mathrm{e}^{-ik_n^{\alpha}(x-x_\alpha)}\right)\\
&\quad\times\cos\frac{n\pi(z-z_{\alpha,\beta})}{b_\alpha}.
\end{aligned}
\tag{3}
$$

The index $\alpha = 1,2,\ldots,5$ corresponds to the individual regions, the index β to the subregions. We have $\beta = 1,2$ for $\alpha = 1$; for $\alpha = 2$ or 4 we have $\beta = 1$ and we can omit it, for $\alpha = 3,5$ we have $\beta = 1,2,\ldots,N_{\mathrm{rod}}+1$. Here

$$
k_n^{\alpha} = \begin{cases} \sqrt{k_{\mathrm{v}}^2 - (\frac{\pi}{a})^2 - (\frac{n\pi}{b_\alpha})^2} & \text{for } n = 0,1,\ldots,N_\alpha^{\mathrm{prop}} \text{ (propagating modes).}\\ i\sqrt{(\frac{\pi}{a})^2 + (\frac{n\pi}{b_\alpha})^2 - k_{\mathrm{v}}^2} & \text{for } n = N_\alpha^{\mathrm{prop}}+1,\ldots \text{ (evanescent modes).}\end{cases}
\tag{4}
$$

For the fundamental mode ($n = 0$) $k_0^{\alpha} = k_0 = \sqrt{k_{\mathrm{v}}^2 - (\frac{\pi}{a})^2}$. We suppose that the number of propagating modes ($1 + N_\alpha^{\mathrm{prop}}$) in the regions {1} ,{2} and {4} is greater than one (hyperguides) but only the fundamental mode propagates in the narrow waveguides in the region {3} and {5} ($N_3^{\mathrm{prop}} = N_5^{\mathrm{prop}} = 0$). The face of the wall separating waveguides {1,1} a {1,2} has the position $x_1 = -(l_1 + l_2 + l_3 + l_4)$. The centres of waveguides {2-4} have the x-coordinates $x_2 = -(\frac{l_1}{2} + l_2 + l_3 + l_4)$, $x_3 = -(\frac{l_2}{2} + l_3 + l_4)$ and $x_4 = -(\frac{l_3}{2} + l_4)$. The main rods start at $x_5 = -l_4$ and end at $x = 0$. The coordinate of the left wall of the $\{\alpha,\beta\}$-th waveguide is $z_{\alpha,\beta} = (\beta - 1)(b_\alpha + d_\alpha)$. We also denote the z-coordinates of the left wall of the $\{\alpha,\beta\}$-th septum separating the waveguides as $\Xi_{\alpha,\beta}$ ($\Xi_{\alpha,\beta} = \beta b_\alpha + (\beta - 1)d_\alpha$).

Because the structure has the unified height a we can confine ourselves to the modes $(1,n)$, ie to the y-dependence of the fields in the form $\sin(\pi y/a)$ in (3). Thus for $n = 0$ we have the fundamental mode TE_{10} which has only the z-component of the electric field. Because the electric field of the incident wave must be perpendicular to the rods we choose, for $n = 1,2,\ldots$, such combinations of the TE_{1n} and TM_{1n} modes that have $E_y \equiv 0$. The form of fields (3) ensures the automatic fulfilment of this condition. It can be proved that if the incident mode does not contain any y-component of the electric field the diffracted and reflected waves have not it either. In the following section, it is described how to excite such a mode in the oversized waveguide.

We do not need the expressions for the remaining tangential components of fields because $E_y \equiv 0$ and the continuity of H_z follows, in this case, from the continuity of E_z and H_y. Thus the only conditions, which must be fulfilled at the discontinuities at x_1 and x_5 (eventually at $x_3 \pm l_2/2$), follow from the continuity of the components E_z and H_y.

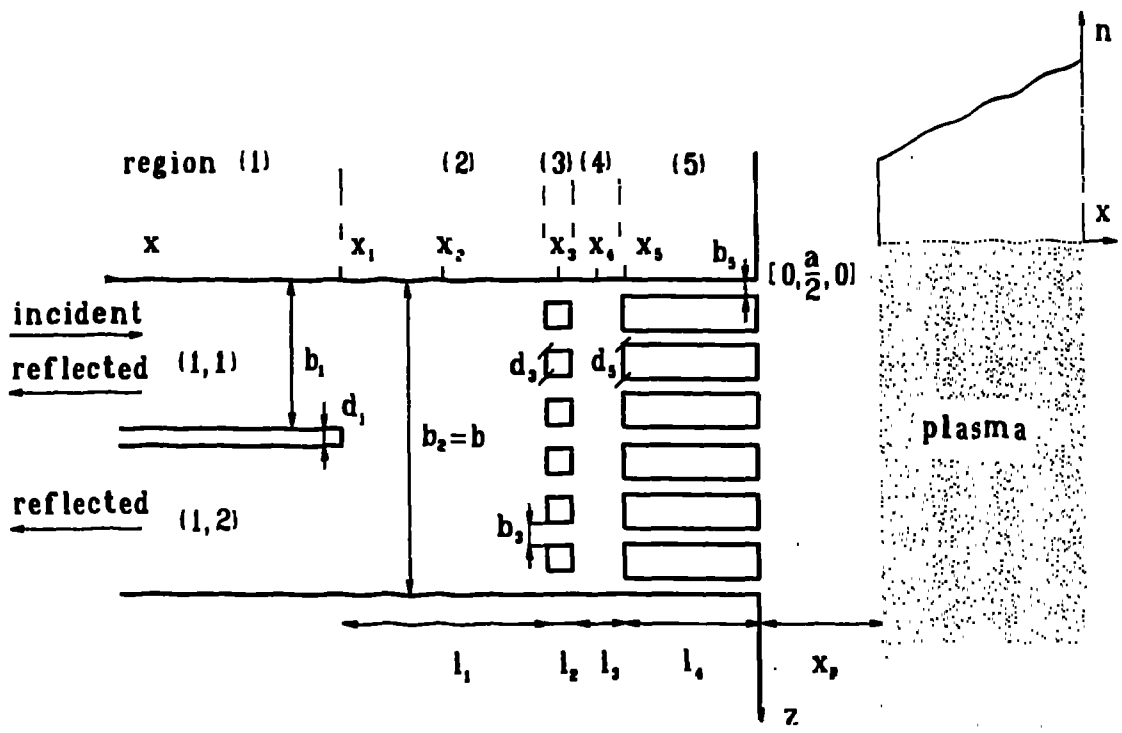

Figure 2: Section through our quasi-optical grill by the plane perpendicular to the rods. Here we indicated five regions in which the solutions (3) are continuous and also all notations used for the structure dimensions. We also depicted the plasma in front of QOG in the distance x_p with the step and ramp density profile.

To fulfil the boundary conditions at $x \to -\infty$ we must set $A_n^{1,\beta} = \delta_{1,\beta}\delta_{n,l_{\rm inc}} A_{l_{\rm inc}}^{1,1}$ for $\beta = 1,2$, $n = 0,1,2,\ldots$, where $l_{\rm inc}$ is the order of the incident mode in the $\{1,1\}$-waveguide and $\delta_{n,m}$ is the Kronecker delta. Because we investigate only the highly elongated rods in the row at the grill mouth, we have $|\, k_n^5 l_4 \,| \gg 1$ for $n = 1,2,\ldots$ and we can set $B_n^{5,\beta} = 0$ for $\beta = 1,2,\ldots,N_{\rm rod}+1$ and $n = 1,2,\ldots$. Thus, we suppose that the power transmission between the interior of the structure and the space in front of the grill is realized through the fundamental mode only. On this assumption we can split the solution of our problem into two parts. First we can compute the transmission and reflection coefficients of our waveguide junction consisting of already mentioned five regions and than we can determine the coupling of the junction through the $(N_{\rm rod}+1)$-waveguide multijunction grill to the plasma.

From the general theory of the waveguide junctions it follows that the amplitudes of waves outgoing from the junction are linear functions of the amplitudes of waves ingoing into the junction [9]. Thus we can express the amplitudes of the waves incident on a plasma in the individual waveguides of the final multijunction section of our structure as

$$A_0^{5,\beta} = \tau_\beta A_{l_{\rm inc}}^{1,1} + \sum_{\gamma=1}^{N_{\rm rod}+1} \rho_{\beta\gamma} B_0^{5,\gamma}, \qquad \beta = 1,2,\ldots,N_{\rm rod}+1. \tag{5}$$

While the transmission coefficients τ_β depend on the order of the incident mode $l_{\rm inc}$ in the feeding waveguide, the reflection coefficients $\rho_{\beta\gamma}$ depend on the geometry of the junction only. Similarly we can write for the amplitudes of reflected waves in the feeding waveguide $\{1,1\}$ and in the passive waveguide $\{1,2\}$

$$B_m^{1,\beta} = \rho_{1,\beta}^m A_{l_{\rm inc}}^{1,1} + \sum_{\gamma=1}^{N_{\rm rod}+1} \tau_{1,\beta\gamma}^m B_0^{5,\gamma}, \quad \beta = 1,2, \quad m = 0,1,2,\ldots,N_1^{\rm prop}. \tag{6}$$

The numerical values of the amplitude reflection and transmission coefficients ($\rho_{\beta\gamma}$, τ_β at $x = x_5$ and $\rho_{1,\beta}^m$, $\tau_{1,\beta\gamma}^m$ at $x = x_1$) can be determined from the continuity conditions of E_z and H_y at all discontinuities of the junction (see (31-34) in Appendix).

Now we discuss the coupling of waves in our structure to a plasma in front of the grill. As was stated the discontinuities at the splitting ($x = x_5$) and at the grill mouth ($x = 0$) can be than solved independently. Waves traveling through the waveguides $\{5,\beta\}$, $\beta = 1,2,\ldots,N_{\rm rod}+1$, gain the same phase shift $\phi_0 = k_0 l_4$ in each waveguide. To simplify the calculation of the grill-plasma coupling we use the parallel-plate waveguide model for the grill mouth. The electric field in the grill mouth can be written as

$$E_z = \sum_{\beta=1}^{N_{\rm rod}+1} \theta_\beta(z) e^{i(\phi_0 - \omega t)} \left(A_\beta e^{ik_v x} + B_\beta e^{-ik_v x} + \text{evan.modes} \right). \tag{7}$$

Here $\theta_\beta(z) = 1$ in the β-th waveguide mouth and 0 elsewhere. Using (5) the amplitudes of the incident waves in the grill mouth can be written in the form

$$A_\beta = \sqrt{\frac{k_0}{2k_v}} \tau_\beta A_{l_{\rm inc}}^{1,1} + \sum_{\gamma=1}^{N_{\rm rod}+1} \rho_{\beta\gamma} e^{2i\phi_0} B_\gamma, \qquad \beta = 1,2,\ldots,N_{\rm rod}+1. \tag{8}$$

The amplitudes (8) have the same form as in the theory of the multijunction grill [7] and thus can be inserted into the Brambilla equations describing the waveguide grill [10]. Solving this system we obtain the amplitudes of the waves reflected from the plasma B_β, the amplitudes of the evanescent modes in the grill mouth and also the amplitudes of the incident waves A_β. We can thus determine the spectra of the waves radiated from our structure into a plasma. The amplitudes $B_0^{5,\beta}$ are given by

$$B_0^{5,\beta} = \sqrt{\frac{2k_v}{k_0}} e^{2i\phi_0} B_\beta. \tag{9}$$

Inserting (9) into (6) we obtain the amplitudes of the reflected waves $B_m^{1,\beta}$.

At the end of this section we write down the explicit expressions for the total time-averaged incident, reflected and transmitted power flows. These global parameters represent the most important results of our theory and, moreover, the conservation of the total power flow can measure the numerical precision of our computation. For the incident power flow $P_x^{\rm inc}$ in the $\{1,1\}$-waveguide we have

$$\begin{aligned} P_x^{\rm inc} &= -\int_0^a dy \int_0^{b_1} dz (\frac{1}{T}\int_0^T (\frac{c}{4\pi}) \Re E_z \Re H_y \, dt \\ &= K_1 \frac{b_1}{2k_{l_{\rm inc}}^1} \mid A_{l_{\rm inc}}^{1,1} \mid^2. \end{aligned} \tag{10}$$

where $K_1 = c(k_0)^2 a/(16\pi k_{\rm v})$ and $T = 2\pi/\omega$. The reflected power flow can be written as

$$P_x^{\rm refl} = K_1 \sum_{\beta=1}^{2} \sum_{m=0}^{N_1^{\rm prop}} \frac{\varepsilon_m b_1}{k_m^1} \mid B_m^{1,\beta} \mid^2, \tag{11}$$

where $\varepsilon_0 = 1$ and $\varepsilon_m = \frac{1}{2}$ for $m > 0$. Finally for the transmitted power we have

$$P_x^{\rm transm} = K_1 \frac{b_5}{k_0} \sum_{\beta=1}^{N_{\rm rod}+1} \left\{ \mid A_0^{5,\beta} \mid^2 - \mid B_0^{5,\beta} \mid^2 \right\}. \tag{12}$$

The power flow conservation asks for the fulfilment of the relation

$$P_x^{\rm transm} = P_x^{\rm inc} - P_x^{\rm refl}. \tag{13}$$

The total power reflection coefficient can be written as

$$R_{\rm tot} = \frac{P_x^{\rm refl}}{P_x^{\rm inc}}. \tag{14}$$

3 Optimization of the quasi-optical grill mounted in the hyperguide

3.1 Structure dimensions and plasma parameters

Now we give a realistic example of QOG mounted in the hyperguide cavity and optimize its dimensions to obtain the structure with as low power reflection and as high directivity of the spectrum as possible. We have chosen the working frequency $f = 9.6\,\mathrm{GHz}$ ($k_{\rm v} = 2.012$, $\lambda_{\rm v} = 3.12\,\mathrm{cm}$). the height of the main hyperguide $a = 8\,\mathrm{cm}$ and its width $b = 7.4\,\mathrm{cm}$. The feeding waveguide has the same height a and the width $b_1 = 3.5\,\mathrm{cm}$. The same dimensions have the passive waveguide and the wall separating them has the thickness $d_1 = 0.4\,\mathrm{cm}$. We assume that the structure has six rods in a row and one or two rows of rods. The other dimensions will be determined during the optimization. Their starting values are given by the estimates stated in

the Introduction. When we change the dimensions of rods and gaps we all the time suppose that $7 \times b_\alpha + 6 \times d_\alpha = b$, for $\alpha = 3, 5$.

We assume that the surface plasma density $n_{\rm surf}$ in front of the grill is higher than the critical density ($n_{\rm surf}/n_{\rm crit} = 1 - 10$). We take the density gradient $\frac{dn}{dz} = 7 \times 10^{11}\,{\rm cm}^{-4}$ but we found that the results are practically insensitive to the value of this parameter if the plasma has the over-critical surface density. Eg for $n_{\rm surf}/n_{\rm crit} = 2$ there is no observable change in the efficiency of the structure for the density gradients in the range from 0 to $2.5 \times 10^{13}\,{\rm cm}^{-4}$.

The smaller variant of the structure ($a = 5.2\,{\rm cm}$, $b = 6.8\,{\rm cm}$) is now assembled in Prague and it will operate at the slightly lower frequency 9.3 GHz at CASTOR tokamak [8]. The plasma parameters used in the optimization fit well with those at CASTOR tokamak but the direct application of the results of our theory is rather questionable because the toroidal magnetic field in CASTOR is low (1.3 T) and the working frequency is too high to fall within the lower hybrid frequency range. The determination of the surface plasma impedance would be complicated here because, in this case, we could not neglect the coupling between the fast and the slow wave in a plasma [11]. On the contrary, in our theory, we use the standard step and ramp plasma surface impedance [12], because we are aimed at the application of our results on the large facilities where the toroidal magnetic field is sufficiently high.

3.2 Incident mode

Now we must specify the incident mode in the feeding waveguide {1,1}. We picked up the (1,1)-mode (ie $l_{\rm inc} = 1$) which has the angle of incidence $\alpha = 27°$ ($k_z = k_1^1 = 0.873 k_{\rm v}$, $k_z = \pi/b_1 = 0.459 k_{\rm v}$, the remaining component k_y is small ($k_y = \pi/a = 0.195 k_{\rm v}$)). The fundamental mode $\rm TE_{10}$ ($k_0 = 0.978 k_{\rm v}$) has proper polarization of the electric field (E_x only) but it is incident perpendicularly on the rods ($k_z = 0$ ie $\alpha = 0$). The last propagating mode (1,2) has the large angle of incidence $\alpha = 66°$ ($k_x = k_2^1 = 0.407 k_{\rm v}$, $k_z = 2\pi/b_1 = 0.918 k_{\rm v}$) and, as a consequence of it, the radiated spectrum contains too much waves with $N_z \approx 1$.

The incident mode (1,1) must have the electric field perpendicular to the rods. To obtain such a polarization the following arrangement can be used. We first split the power from the generator into two one mode auxiliary standard waveguides (in our case $2.3 \times 1\,{\rm cm}$) and excite there the $\rm TE_{10}$ modes to be in antiphase. Than we enlarge continuously the dimensions of waveguides (in some horn-like sections) to the desired $a \times (b_1 - d_1)/2$. Because, in our case, $(b_1 - d_1)/2 = 1.55\,{\rm cm}$ and, therefore, it is smaller than the half vacuum wavelength, only the $\rm TE_{m0}$ modes can propagate in these waveguides. Further, if we take the length L of this horn-like widening sufficiently long, only the $\rm TE_{10}$ modes are exited in the enlarged auxiliary waveguides. From the the geometrical optics it follows that $L \approx a k_{\rm v}(a - a_{\rm standard})/\pi$, ie $L = 30\,{\rm cm}$. Now, if we put one waveguide on the other by the long sides and if we cancel the septum between them at some distance from the horn-like section we obtain the waveguide $a \times b_1$ in which the mode (1,1) of the desired polarization is excited. The numerical verification confirms that this junction converts two $\rm TE_{10}$ modes in antiphase into one (1,1)-mode with practically 100% efficiency.

3.3 Parameters describing the directivity and efficiency

To be able to compare individual structures and to distinguish which of them are the most efficient we can use the total reflection coefficient (14) and either directly the power spectra or some global parameters derived from them. We introduce three parameters describing the directivity or current drive efficiency. The most simple is the coupled power directivity

$$\delta_{\mathrm{CP}} = \int_{-\infty}^{-1} G(N_z)\, dN_z. \tag{15}$$

where N_z is the parallel wave index, $G(N_z)$ is the normalized spectral density of the power radiated from the structure to the plasma ($\int_{-\infty}^{\infty} G(N_z)\, dN_z = 1$ and $G(N_z)$ is defined eg in [13]). This quantity determines how much power is radiated in the useful direction (the (-z)-direction in our case, because the waves with $s = -1$ are the most important in (2)). Such quantity was used in [4] to estimate the directivity of QOG but, because it is related to the coupled power only, it does not give the full information about the actual current drive efficiency of the specific structure.

As a more useful parameter can serve the standard current drive directivity $\delta^{\mathrm{s}}_{\mathrm{CD}}$ given by

$$\delta^{\mathrm{s}}_{\mathrm{CD}} = (1 - R_{\mathrm{tot}}) \left\{ \int_{1}^{\infty} G(N_z)\, dN_z - \int_{-\infty}^{-1} G(N_z)\, dN_z \right\}. \tag{16}$$

This quantity is negative for our spectra because the power is radiated predominantly in the (-z)-direction.

As the best estimate of the current drive directivity of the spectrum can be used the "$N_{\parallel}$-weighted directivity" based on the theoretical current drive efficiency of waves [14]. In our case we define it as

$$\delta^{\mathrm{w}}_{\mathrm{CD}} = (1 - R_{\mathrm{tot}})(N_z^{\mathrm{peak}})^2 \left\{ \int_{1+\Delta}^{\infty} \frac{G(N_z)}{N_z^2}\, dN_z - \int_{-\infty}^{-1-\Delta} \frac{G(N_z)}{N_z^2}\, dN_z \right\}. \tag{17}$$

Here N_z^{peak} is the value of the parallel wave index at the $s = -1$ peak of the power spectrum. We introduce a small parameter Δ to cut the fast waves off from our spectra. The spectrum of QOG contains too much waves with $N_z \approx \pm 1$ which can spoil the resulting directivity. This is caused by the presence of waves corresponding to the zero order peak in (2). It is placed in the forbidden band of wavelength in the plasma, but the Floquet's theorem is strictly valid for the infinite structures only, where the peaks have a form of the δ-functions [15]. For our structure the peaks have a finite width and the wings of the peaks can leak out from the forbidden band. We set $\Delta = 0.15$ and thus we exclude the resonant electrons with the energies larger then 0.5 MeV from our considerations.

Finally, to optimize our structure, we introduce the power transmission efficiency η_{PT} [16]. The incident and reflected powers, P_l^{inc} and P_l^{refl}, in the waveguides of the final multijunction section of our structure are distributed highly unevenly and this parameter can help to determine the maximum feeding power for which we keep below the electric breakdown in the most overloaded waveguide. Such a parameter

can be defined as

$$\eta_{PT} = \min_{l=1,2,\ldots,N_{rod}+1} \frac{P_x^{inc}}{(N_{rod}+1)\left(\sqrt{P_l^{inc}} + \sqrt{P_l^{refl}}\right)^2}. \qquad (18)$$

In the ideal case ($\eta_{PT} = 1$) we have no reflected powers and the incident ones equal to 1/7 of the total incident power.

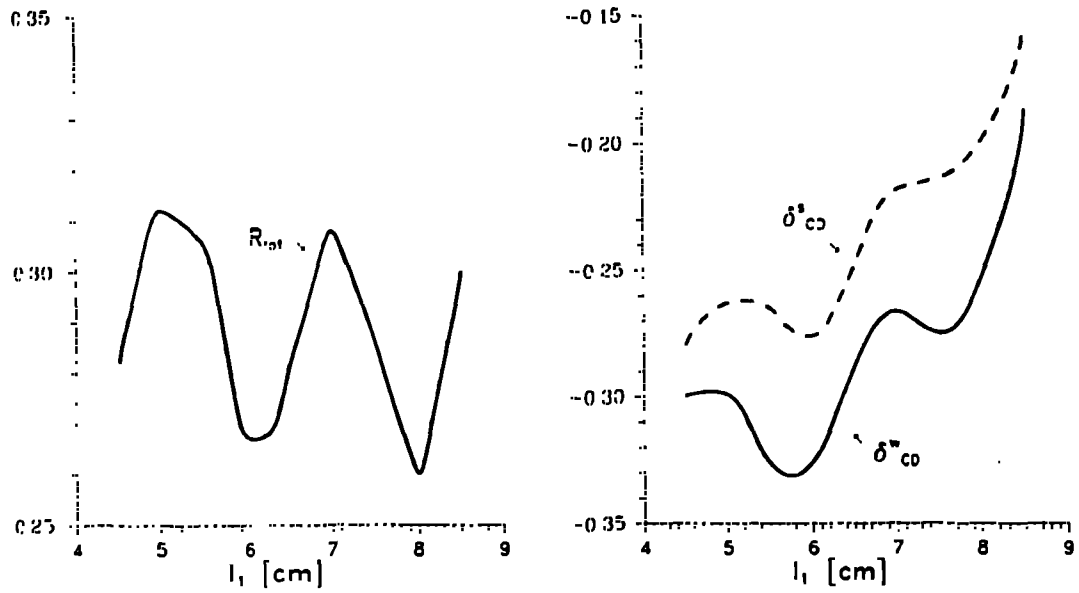

Figure 3: Power reflection coefficient, standard and weighted directivities vs distance l_1 between the mouth of the active auxiliary waveguide and the row of rods. The one row of six rods is supposed and the (1,1)-mode is incident in {1.1}-waveguide ($\alpha = 27°$). The optimum irradiation of rods is reached at $l_1 = 6\,$cm. The other parameters are: the working frequency $f = 9.6$ GHz, the structure dimensions $a = 8\,$cm, $b_1 = 3.4\,$cm, $d_1 = 0.4\,$cm, $d_5 = 0.79875\,$cm, $l_4 = 3.18\,$cm, the distance between plasma and the grill mouth $x_p = 0.124\,$cm and the plasma parameters are $n_{surf} = 4n_{crit}$ and $\frac{dn}{dx} = 7 \times 10^{11}\,\mathrm{cm}^{-4}$.

3.4 One row of rods

We shall suppose that the structure consists of one row of rods, ie we set $l_2 = l_3 = 0$, $A_n^4 \equiv A_n^2$ and $s_n^4 \equiv s_n^2$ in (31,32).

To optimize this problem in a general way is very difficult because it depends on many parameters. Thus, we first fix several of them (the frequency, the order of the incident mode, the dimensions of the main hyperguide, the thickness of the wall separating the active and passive auxiliary waveguides, the distance of the plasma from the grill mouth, the surface plasma density and the density gradient) and then we attempt to reach the optimum by changing one of the remaining parameters while the rest of them is kept fixed. The independence of the physical processes underlining the determination of the optimum explains the success of this procedure.

The optimum distance l_1 giving the best irradiation of rods is determined only by the geometry of the main waveguide. From Fig. 3 we see that the power reflection coefficient and both the standard and weighted directivities have the optimum at $l_1 = 6\,\mathrm{cm}$. This distance is about 17% shorter then the estimate based on the geometrical optics given in the Introduction. It can be explained by the inadequacy of the GO in our case in which the diffraction plays an important role. It is confirmed

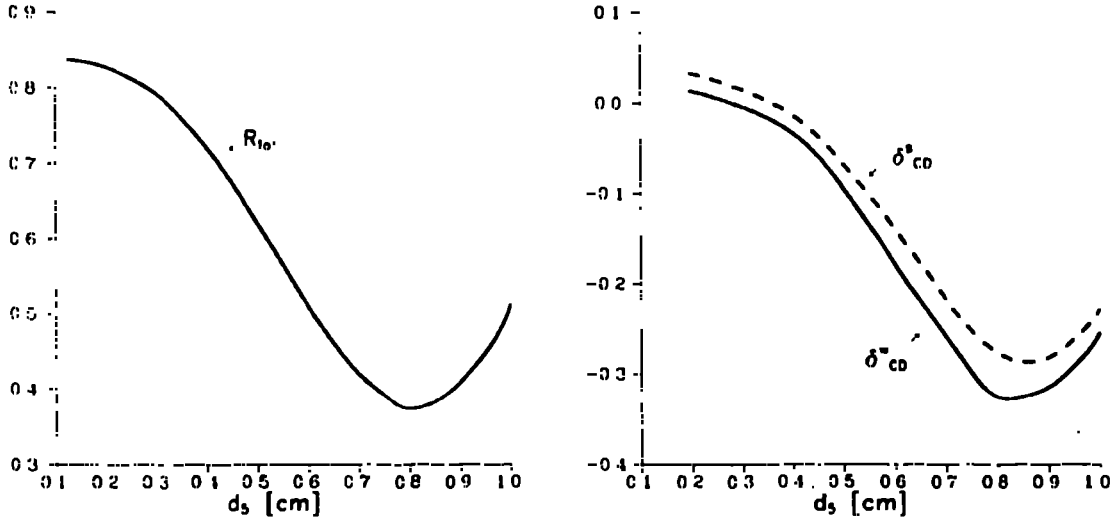

Figure 4: Power reflection coefficient, standard and weighted directivities vs thickness d_5 of the rods. The optimum diffraction is obtained for $d_5 \approx 0.8\,\mathrm{cm}$. We use $l_1 = 6\,\mathrm{cm}$ and the other parameters are given at Fig. 3.

also by the optimization of the smaller structure where this discrepancy is higher because GO works here even worse. In the process of the optimization we also paid an attention to the distribution of the incident powers in the waveguides of the final multijunction section. If l_1 is too short the power in the {5,1}-waveguide is too high, if, in turn, l_1 is too long the same is true for the {5,7}-waveguide. We also examined the power spectra and observed the parasitic peaks corresponding to the wave with

($-k_z$) for both the shorter l_1 than optimum and the longer one.

The optimum for the thickness d_5 of the rods follows from the compromise between the substantial diffraction of waves, which calls for the huge rods, and the broad gaps through which waves can well penetrate. From Fig. 4 we see that the rods must have the thickness equal $\lambda_v/4$ to be effective. There is a slight dependence of the optimum d_5 on the surface density and we use $d_5 = 0.8\,\text{cm}$ which works well for the higher surface density ($n_{\text{surf}} = 4n_{\text{crit}}$). The gap between the rods is narrow ($b_5 = 0.37\,\text{cm}$).

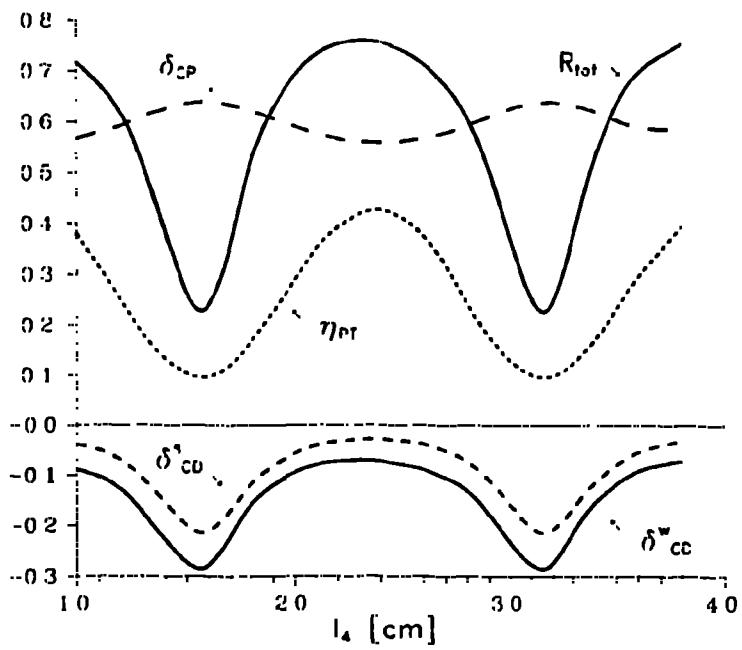

Figure 5: Directivities, power reflection coefficient and power transmission efficiency vs length l_4 of rods (the length of the waveguides of the multijunction section). The optimum is reached at resonance values $l_4 = n \times 1.592\,\text{cm}$, $n = 1, 2, \ldots$. Only the values of η_{PT} are unsatisfactory here. We use $l_1 = 6\,\text{cm}$, $x_p = 0.0745\,\text{cm}$, $n_{\text{surf}} = 2n_{\text{crit}}$ and the other parameters are given at Fig. 3.

The impressive picture of the resonant behavior of all interesting quantities gives the dependence of the power reflection coefficient, directivities and power transmission efficiency on the length l_4 of the rod cross-section (see Fig. 5). The resonances occur at the exact multiples of the half wavelength of the fundamental mode ($\lambda_0 = 2\pi/k_0 = 3.184\,\text{cm}$ in our case). All quantities manifest also the full periodicity with respect to this quantity, because the length l_4 enters into our calculations only through the factor $e^{2i\phi_0}$ (see (8-9)). Thus the same results can be obtained for $l_4 = 1.592\,\text{cm}$ but we used $l_4 = 3.184\,\text{cm}$ to separate well the junction problem from the coupling problem.

The reflection coefficient decreases and the directivity (in the absolute value) increases substantially in the resonance region but, at the same time, the power transmission efficiency falls. The main cause is the formation of the strong standing waves in the separate waveguides of the terminal multijunction section (see Fig. 6). The same but much weaker effect was observed at the standard multijunction grill [17] in which the non-zero phase shifts between the adjacent waveguides prevent the waveguides from being resonant all at once. We suppose that the large structures with many rods can be optimized with respect of η_{PT} by an uneven distribution of the incident power in several feeding waveguides.

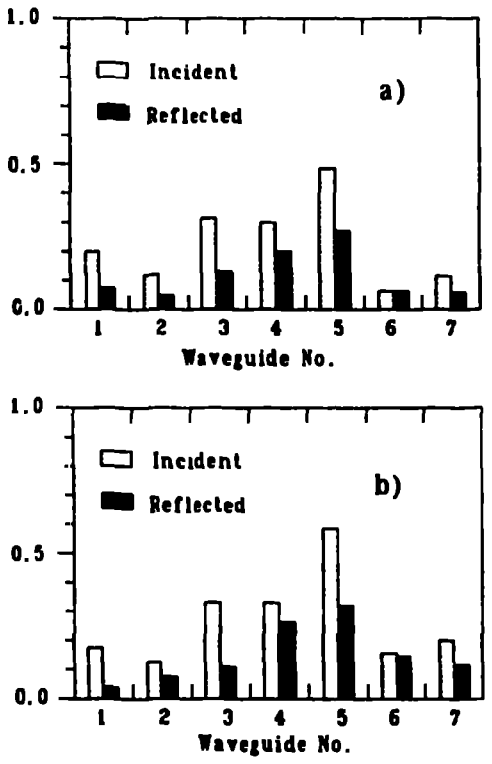

Figure 6: Distribution of the incident and reflected powers (divided by the total incident power) in the individual waveguides of the multijunction grill formed by the gaps between the rods. The fifth waveguide is highly overloaded and the incident powers are distributed highly non-uniformly. The case a) one row of rods (η_{PT} = 0.0962) and the same parameters as in Fig. 5; b) the parameters correspond to the optimum structure with two rows of rods with the spectrum given in Fig. 14 ($\eta_{PT} = 0.0806$).

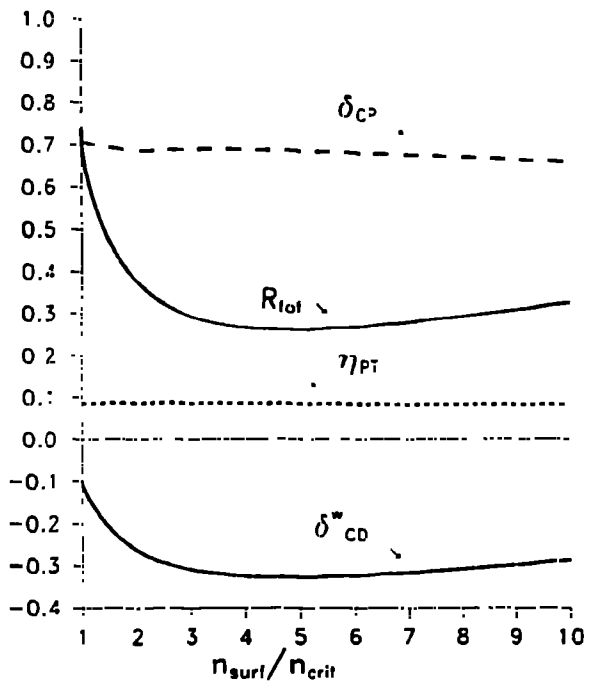

Figure 7: Directivities, power reflection coefficient and power transmission efficiency vs surface plasma density. The same parameters as in Fig. 3 with the optimum $l_1 = 6\,\mathrm{cm}$.

The best coupling of the waves in our structure to the waves in a plasma is reached for $n_{surf} = (2-6)n_{crit}$ (see Figs. 7 and 9). In the rarefied plasma with the $n_{surf} < n_{crit}$ the structure cesses to operate.

The quasi-optical grills are very sensitive to the distance between the grill mouth and the plasma (see Fig. 8). The standard directivity is very low at $x_p = 0$ and also the absolute value of the weighted directivity decreases here, the both quantities reach the optimum for $x_p = 1 - 2\,\mathrm{mm}$. This behavior can be understood from the dependence of the spectral power density on x_p and N_z. For $|N_z| > 2$ we can approximate $G(N_z)$ as

$$G(N_z) = e^{-2k_v x_p |N_z|} \frac{|\,D(N_z)\,|^2}{|N_z|}. \qquad (19)$$

where $D(N_z)$ is the Fourier transform of the z-component of the electric field E_z and its absolute value is symmetrical with respect to $N_z = N_z^{inc}$. As x_p grows the short wavelength waves cannot get over the vacuum gap and the spectrum consists mainly of the waves corresponding to the $s = -1$ peak. But at the same time the the power reflection coefficient sharply increases and, at the higher x_p. the undesirable waves with $|N_z| \approx 1$ appear in the spectrum. Thus the directivity has the optimum at some small but finite x_p.

In Fig. 9 we show that this optimum x_p shifts slightly to the higher values as the surface plasma density grows. At low densities the optimum x_p is practically equal

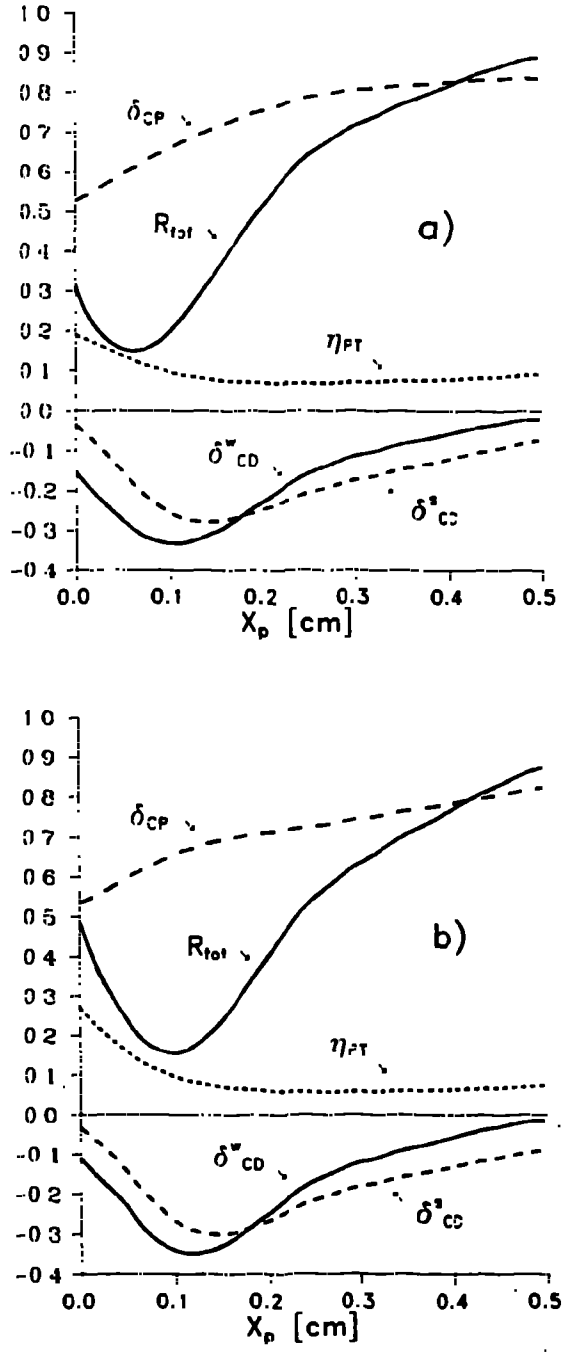

Figure 8: Directivities, power reflection coefficient and power transmission efficiency vs distance x_p between the grill mouth and the plasma. The case a) the structure with one row of rods and the same parameters as at Fig. 3; b) two rows of rods with the parameters given in Fig. 14.

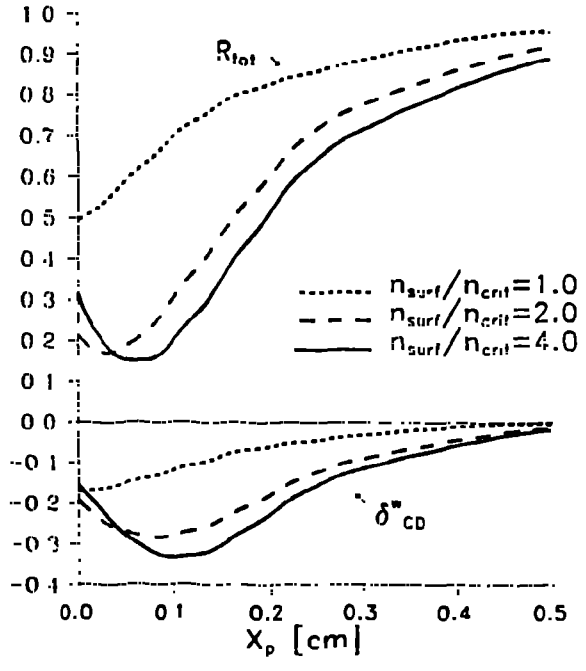

Figure 9: Power reflection coefficient and weighted directivity vs the distance x_p between the grill mouth and the plasma for several surface plasma densities. The same parameters as at Fig. 3 with the optimum $l_1 = 6\,\mathrm{cm}$.

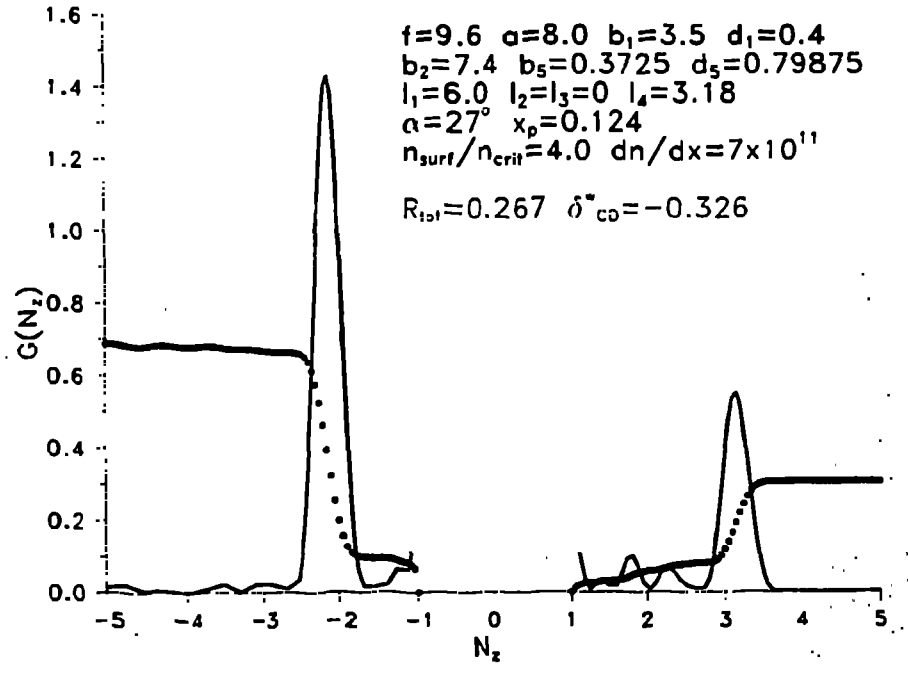

Figure 10: Power spectrum of the optimized six rod quasi-optical grill mounted in the hyperguide. The curves composed from "*" represent the integrals $\int_{\pm 1}^{\pm N_z} G(N_z)\, dN_z$.

The power spectrum for the optimum structure and plasma parameters is shown in Fig. 10. The left peak ($N_z = -2.15$) corresponds to the $s = -1$ diffraction order in (2), the right one ($N_z = -3.15$), corresponding to $s = 1$, is parasitic and its presence diminish the resulting directivity. The positions of peaks coincide well with the predicted ones on the basis of the Floquet's theorem. The curves made of "*" represent the integrals $\int_{\pm 1}^{\pm N_z} G(N_z)\, dN_z$ and they can be used to estimate how much power an individual peak contains.

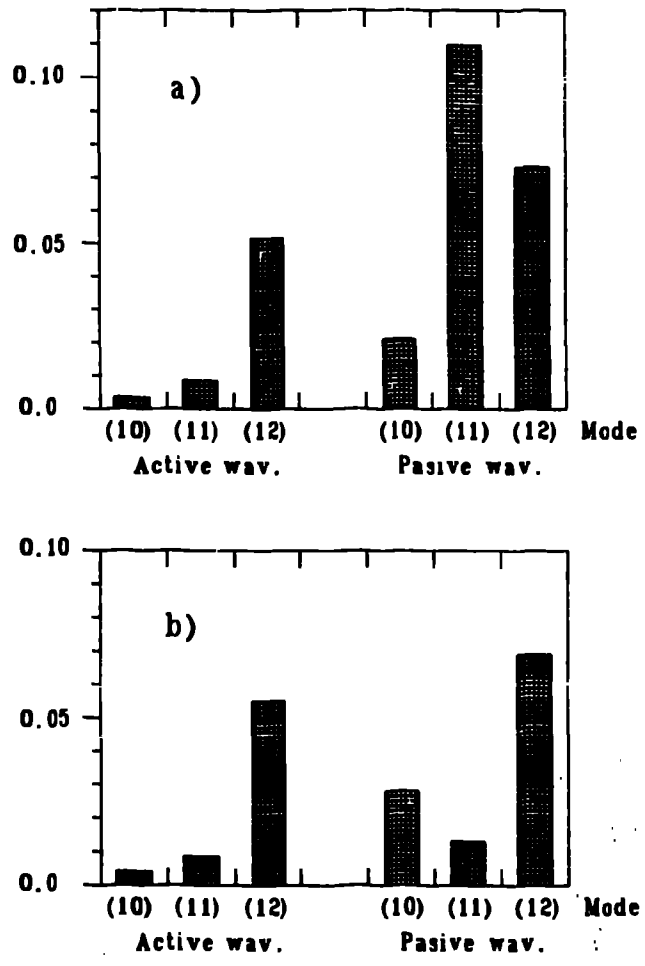

Figure 11: Distribution of the normalized reflected powers between the auxiliary waveguides {1,1} and {1,2} and three propagating modes. The case a) corresponds to the optimized structure with six rods in one row having the spectrum depicted in Fig. 10. The case b) corresponds to the optimized structure with two rows of rods having the spectrum depicted in Fig. 14.

The waves are reflected predominantly into the passive auxiliary waveguide {1,2} in the form of the (1,1)- and (1,2)-modes (see Fig. 11a). The reflected waves in

the active waveguide consist practically of the (1,2)-mode which cannot be easily damped here and it is partly reflected back to the rods. In the present paper we neglect this reflection.

3.5 Two rows of rods

The second auxiliary row of rods can improve irradiation of the main row of rods situated in the grill mouth. In the course of optimization we found that the proper irradiation of the main row of rods can be achieved only if the sum of the distance l_1 from the junction of the auxiliary waveguides to the auxiliary row and the distance l_3 from the auxiliary row to the main row is equal to the value obtained in the optimization of the structure with one row of rods only, ie $l_1 + l_3 = 6\,\mathrm{cm}$ in our case. We also found that the magnitude of l_2, ie the length of the auxiliary rods in the direction of the wave propagation, has very small influence on the optimum. Thus we suppose that these rods have the square cross-section, ie $l_2 = d_3$.

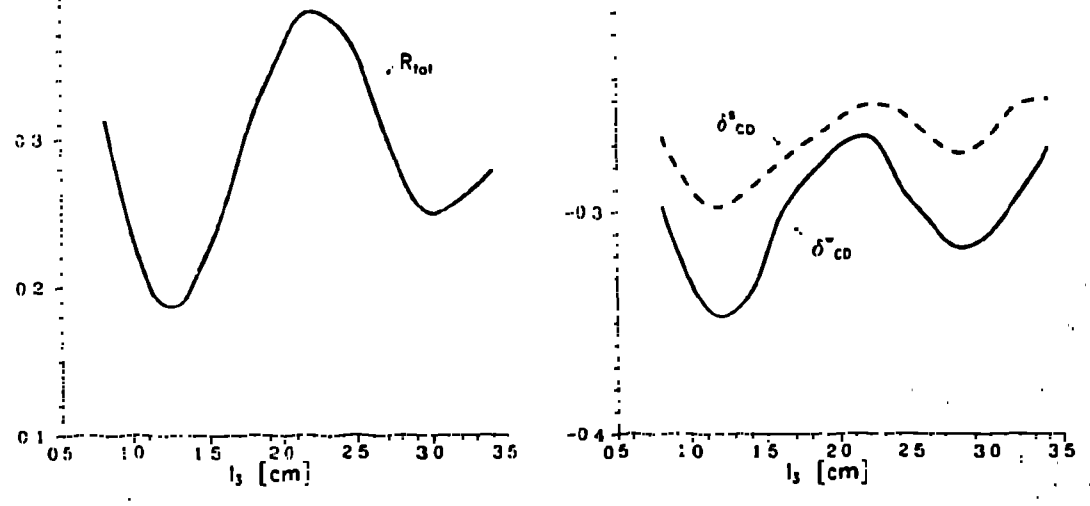

Figure 12: Power reflection coefficient, standard and weighted directivities vs distance l_3 between the auxiliary row and the main row of rods. The six rods in each row is considered. The optimum is reached at $l_3 = 1.2\,\mathrm{cm}$. We suppose the optimum $l_1 + l_3 = 6\,\mathrm{cm}$, $l_2 = d_3$ and $d_3 = 0.51\,\mathrm{cm}$ and the same parameters as at Fig. 3.

The optimum distance between the auxiliary and the main rows is reached at the slightly shorter distance than gives the condition of the constructive superposition of the incident and doubly reflected waves. In our case, the optimum $l_3 = 1.2\,\mathrm{cm}$ (see Fig. 12) is lower than the estimate from the Introduction which gives $l_3 = 1.42\,\mathrm{cm}$.

The second optimum at $l_3 = 2.9\,\mathrm{cm}$ in Fig. 12 is inferior to the first because the first row is too close to the mouth of the feeding auxiliary waveguide in this case.

The described optimum differs from the optimum resonance distance between rows found by M.I. Petelin [3] for QOG in a free space or used in the design of the new QOG for TORE SUPRA [19]. This resonance distance D is determined by the condition $k_x D = \pi$ and corresponds to excitation of the travelling TM_1 mode in the parallel-plate waveguide formed by two rows of rods ($E_z \sim \sin(\pi x/D)e^{ik_z z}$, $E_x \sim (ik_z/k_x)\cos(\pi x/D)e^{ik_z z}$). Such a mode can exists only if nothing prevents the waves from propagating freely along the rows of rods (in the z-direction). If the quasi-optical grill is immersed into the cavity the travelling modes should be converted into the eigenmodes of the closed resonator ($E_z \sim \sin(\pi y/a)\sin(k_n^2 x)\cos(n\pi z/b), n = 1,2,3,4$) but from Fig. 12 it seems that no eigenmodes are excited at all. The eigenmodes ought to have the negative effect on the directivity and the decrease of R_{tot} at $l_3 = 3$ can be attributed rather to the fulfilment of the condition $l_3 = \lambda_0 \cos\alpha = 2.8$ than the resonance of the fourth mode ($D_4 = \pi/k_4^2 = 3.12$). We tested, with negative result, the problem of eigenmodes on the case when we kept $l_1 = 6\,\mathrm{cm}$ (the optimum irradiation of the auxiliary row of rods) and changed the distance l_3 from $1 - 4\,\mathrm{cm}$.

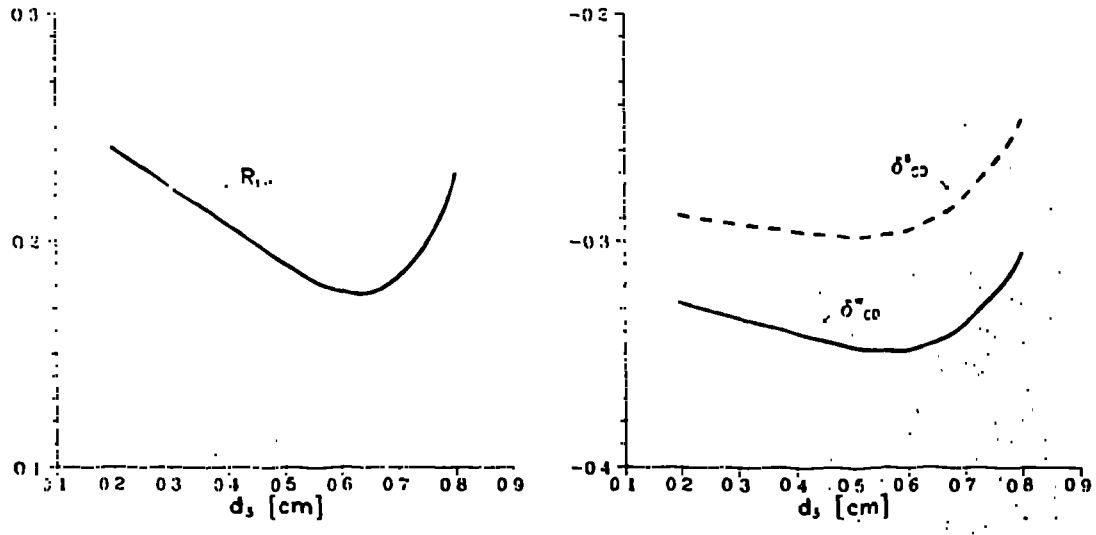

Figure 13: Power reflection coefficient, standard and weighted directivities vs thickness d_3 of the auxiliary rods. The optimum diffraction is obtained for $d_3 \approx 0.6\,\mathrm{cm}$. We use $l_1 = 4.8\,\mathrm{cm}$, $l_3 = 1.2\,\mathrm{cm}$ and the other parameters are given at Fig. 3.

The optimum thickness d_3 of the rods of the auxiliary row is slightly below $\lambda_v/4$. From Fig. 13 we see that $d_3 = 0.6\,\mathrm{cm}$.

From Fig. 8b it follows that the optimum distances x_p for the weighted directivity and for the power reflection coefficient practically coincide for the two row structure. This explains the lower reflection at the optimum in this case. On the contrary, for one row structure (Fig. 8a), the minimum of the reflection coefficient is shifted with respect to maximum of $|\delta^{b}_{CD}|$ to the lower x_p.

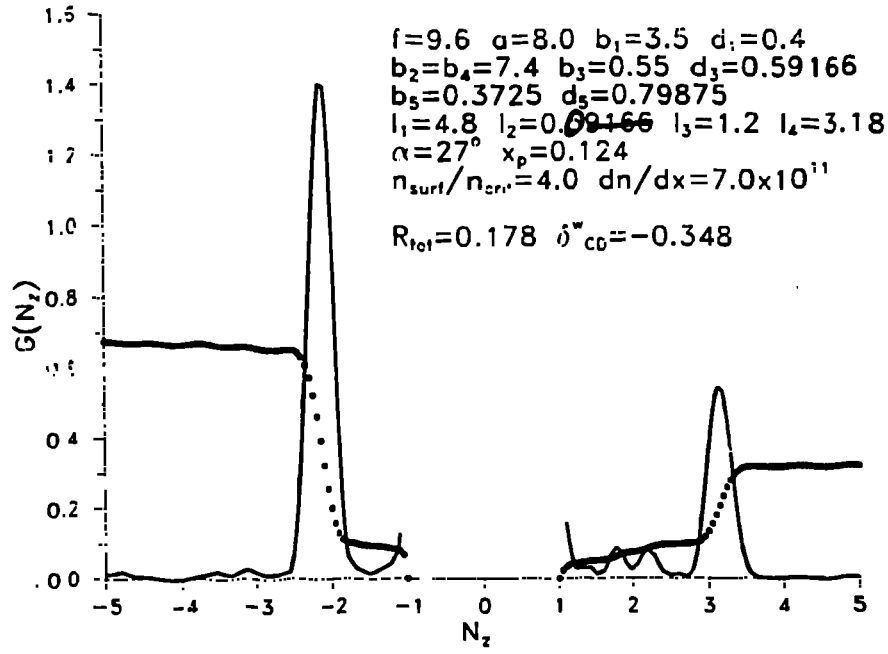

Figure 14: Power spectrum of the optimized quasi-optical grill consisting of two rows of rods mounted in the hyperguide. Each of rows has six rods.

The power spectrum for the fully optimized structure with two rows (each having six rods) is given in Fig. 14. The spectrum has practically the same shape as in the case of the one row structure (see Fig. 10) but the reflection coefficient is smaller and the directivity is slightly better.

The second row improves the distribution of the incident powers in the the waveguides of the final multijunction section (the main row of rods) which is depicted in Fig. 6b (waveguides 1,2,6,7), but the overloading of the central waveguides is stronger than that in the case of one row ($\eta_{PT} = 0.0854$ for one row and $n_{surf} = 4n_{crit}$).

The reflected power of the two row structure does not contain practically any (1,1)-mode as it is seen from Fig. 11b. The second row prevents this mode from escaping the space between rows and thus it is radiated into the plasma. This explains the lower reflection of the two rows structure.

We could continue with the optimization of the second row by several different methods. It is possible to shift the row as a whole about a small distance in the z-direction to change the irradiation of the rods. It is also possible to use the rods

with different thickness and change the width of gaps between them irregularly to achieve a better distribution of the incident and reflected powers in the individual waveguides of the final multijunction section and suppress the overloading of the central waveguides. In the present paper we confine to the simple optimization described in the first paragraph of this section.

3.6 Computation precision

In the one row case we use about 75 modes at each discontinuity, ie we finally solve the set 150 equations to obtain the transmission and reflection coefficients (31-34). The power flow (13) is conserved to four digits. When we solve the coupling problem we use 7 modes per each waveguide and we also compare the power flow in the plasma obtained by the integration of the power spectrum with the transmitted power flow (12); we found that both values fit well to the same precision.

Two row problem has four discontinuities and asks for the solution of 300 equations. The resulting precision of the power flow conservation is only 1% in this case.

4 Conclusions

From the preceding discussion and numerical calculations it seems that the our design of the quasi-optical grill mounted in the large waveguide cavity could be a powerful alternative launcher of the lower hybrid waves for the current drive in large thermonuclear facilities. We revealed several important facts about QOG mounted in a oversized waveguide

- The conducting walls surrounding our QOG do not prevent the rods from being irradiated properly. This is not true for all such structures, eg the confining walls distort the form of wave, if the rods are irradiated by the parabolic mirror [6].

- The resonant length l_4 of the cross-section of the main row rods (in the direction of the wave propagation) ensures that the structure even with one row of rods is highly efficient ($R_{tot} = 0.2$, $\delta_{CP} = 0.7$, $\delta^*_{CD} = -0.3$). This resonant length of rods must give the same excellent results also for the structures operating in a free space. This fact was overlooked in [18] (the authors does not reach the resonant elongation) but it seems that the preliminary proposal of the new QOG for TORE SUPRA working at 8 GHz [19] envisages it.

- The overloading of our structure is not so severe as for the structures with the resonant distance between two rows of rods. In [5] the estimated electric field is 35 higher than the ideal one; for the new QOG with the horn and mirror arrangement [19] the estimate gives the factor 4-5. For our structure $\eta_{PT} = 0.1$, ie the electric field is only 3 times higher then the ideal one.

- The second row of rods improves the efficiency of our structure ($R_{tot} = 0.15$, $\delta_{CP} = 0.7$, $\delta^{w}_{CD} = -0.35$) but we do not confirmed the existence of the resonance distance between rows of rods for the structure bounded by the conducting walls.

- The structure has $(3 \times a/\lambda_v)$-times less construction elements than MJG.

We can compare our structure with the waveguide grills described in the survey [20]. The big multijunction grills have the weighted directivity about 50%, the power reflection coefficient about 5% and the peaking factor on the electric field equal 2. If we consider, that our structure has only 6 rods and serves as an example how such a structure can operate, our results seem to be very promising. The lower weighted directivity of QOG has two main reasons: the long wavelength parasitic peak and the presence of the waves with $N_z = \pm 1$ in the spectrum. The directivity of large structures could be better, because the width of the peaks in the power spectrum decreases with the increasing number of rods and thus the leaking of waves with $N_z = \pm 1$ is reduced. The limiting power density increases with the grow of applied frequency so that the waveguide overloading need not be so severe.

There are two ways how to create a large structure. We may simple arrange several units (eg having about 10 rods in one row and placed in the separate hyperguide) side by side in one row. The incident waves must be properly phased. This configuration resembles the multijunction arrays. We may also create one big hyperguide with several tens of rods in one row. To irradiate them properly we can use several feeding waveguides, in each of them the properly polarized and phased higher mode is incident. The feeding waveguides fill one half of the common hyperguide (the second half forms an passive structure which absorbs the reflected power) and the walls between them retreat subsequently from rods forming the triangular structure - echelette - which irradiates the rods obliquely by the plane wave. Such a structure resemble the original proposal of the quasi-optical grill and it could have a larger flexibility than the preceding one.

Appendix

DETERMINATION OF THE TRANSMISSION AND REFLECTION COEFFICIENTS OF THE JUNCTION

First, we derive the set of the linear equations for the amplitudes of both propagating and evanescent modes in our structure. The method which we use here was adopted successfully for the solution of the discontinuities in waveguides by R. Mitra and S.W. Lee [21]. The same method proved to be useful in the theory of the multijunction grill [7].

The tangential components of the electric and magnetic fields must be continuos at the discontinuities at x_1, $x_3 \pm l_2/2$ and x_5. Moreover E_z must be equal to zero on

the faces of all rods and walls. The continuity conditions in the z-representation do not suit well for the numerical solution and must be Fourier analyzed. If we exclude the unknown amplitudes $B_m^{1,\beta}$, $A_m^{3,\beta}$, $B_m^{3,\beta}$ and $A_m^{5,\beta}$ we obtain the set of the linear equations for the unknown amplitudes A_m^2, B_m^2 and A_m^4, B_m^4 of modes in the main hyperguide. A_n^2, B_n^2, etc are the abbreviated notations for $A_n^{2,1}$, $B_n^{2,1}$, etc.

From the continuity conditions at $x = x_1$ we have

$$\sum_{n=0}^{N_{\rm tot}-1}\left(A_n^2 s_n^2(1+\frac{k_l^1}{k_n^2})+\frac{B_n^2}{s_n^2}(1-\frac{k_l^1}{k_n^2})\right)R^{1,\beta}(n,l) \;=\; 2\delta_{l,l_{\rm inc}}\delta_{1,\beta}\varepsilon_l A_{l_{\rm inc}}^{1,1},$$
$$\beta = 1,2, \quad l = 0,1,2,\ldots,N_{1w}-1, \tag{20}$$

where $s_n^2 = e^{-ik_n^2 l_1/2}$, N_{1w} is the number of modes in the waveguides $\{1,\beta\}$, $N_{\rm tot}$ is the number of modes in the connecting oversized waveguide $\{2\}$ and the Fourier coefficients

$$R^{\alpha,\beta}(n,l) = \frac{1}{b_\alpha}\int_{z_{\alpha,\beta}}^{z_{\alpha,\beta}+b_\alpha}\cos\frac{n\pi z}{b}\cos\frac{l\pi(z-z_{\alpha,\beta})}{b_\alpha}\,dz. \tag{21}$$

The condition $E_z = 0$ on the face of the wall separating the waveguides $\{1,1\}$ and $\{1,2\}$ gives

$$\sum_{n=0}^{N_{\rm tot}-1}\left(A_n^2 s_n^2+\frac{B_n^2}{s_n^2}\right)R^{1,1}(n,l) \;=\; 0. \qquad l = 0,1,2,\ldots,N_{1f}-1, \tag{22}$$

where N_{1f} is the number of modes on the face of the wall separating waveguides and the Fourier coefficients

$$\bar{R}^{\alpha,\beta}(n,l) = \frac{1}{d_\alpha}\int_{\bar{z}_{\alpha,\beta}}^{\bar{z}_{\alpha,\beta}+d_\alpha}\cos\frac{n\pi z}{b}\cos\frac{l\pi(z-\bar{z}_{\alpha,\beta})}{d_\alpha}\,dz. \tag{23}$$

The continuity conditions at $x = x_3 \pm l_2/2$ gives

$$\sum_{n=0}^{N_{\rm tot}-1}\left(\frac{A_n^2}{s_n^2}(1-\frac{k_l^3}{k_n^2})+B_n^2 s_n^2(1+\frac{k_l^3}{k_n^2})\right)s_l^3 R^{3,\beta}(n,l) -$$
$$\sum_{n=0}^{N_{\rm tot}-1}\left(A_n^4 s_n^4(1-\frac{k_l^3}{k_n^2})+\frac{B_n^4}{s_n^4}(1+\frac{k_l^3}{k_n^2})\right)\frac{R^{3,\beta}(n,l)}{s_l^3} \;=\; 0,$$
$$\sum_{n=0}^{N_{\rm tot}-1}\left(\frac{A_n^2}{s_n^2}(1+\frac{k_l^3}{k_n^2})+B_n^2 s_n^2(1-\frac{k_l^3}{k_n^2})\right)\frac{R^{3,\beta}(n,l)}{s_l^3} -$$
$$\sum_{n=0}^{N_{\rm tot}-1}\left(A_n^4 s_n^4(1+\frac{k_l^3}{k_n^2})+\frac{B_n^4}{s_n^4}(1-\frac{k_l^3}{k_n^2})\right)s_l^3 R^{3,\beta}(n,l) \;=\; 0,$$
$$\beta = 1,2,\ldots,N_{\rm rod}+1 \quad l = 0,1,2,\ldots,N_{3w}-1. \tag{24}$$

where $s_n^3 = e^{-ik_n^3 l_2/2}$, $s_n^4 = e^{-ik_n^2 l_3/2}$ and N_{3w} is the number of modes in the waveguides $\{3,\beta\}$.

The condition $E_z = 0$ on the faces of the rods at $x_3 \pm l_2/2$ gives

$$\sum_{n=0}^{N_{\rm tot}-1}\left(\frac{A_n^2}{s_n^2}+B_n^2 s_n^2\right)\bar{R}^{3,\beta}(n,l) \;=\; 0. \quad \beta = 1,2,\ldots,N_{\rm rod}$$
$$\sum_{n=0}^{N_{\rm tot}-1}\left(A_n^4 s_n^4+\frac{B_n^4}{s_n^4}\right)\bar{R}^{3,\beta}(n,l) \;=\; 0. \quad l = 0,1,2,\ldots,N_{3f}-1. \tag{25}$$

where N_{3f} is the number of modes on the faces of rods at $x_3 \pm l_2/2$.

The continuity conditions at $x = x_5$ gives

$$\sum_{n=0}^{N_{\rm tot}-1} \left(\frac{A_n^4}{s_n^4}(1 - \frac{k_l^5}{k_n^2}) + B_n^4 s_n^4 (1 + \frac{k_l^5}{k_n^2}) \right) R^{5,\beta}(n,l) \;=\; 2\delta_{l,0} B_0^{5,\beta},$$
$$\beta = 1,2,\ldots,N_{\rm rod}+1, \quad l = 0,1,2,\ldots,N_{5w}-1, \tag{26}$$

where N_{5w} is the number of modes in the waveguides $\{5,\beta\}$ of the final multijunction grill.

The condition $E_z = 0$ on the faces of rods of the main row at $x = x_5$ gives

$$\sum_{n=0}^{N_{\rm tot}-1} \left(\frac{A_n^4}{s_n^4} + B_n^4 s_n^4 \right) \tilde{R}^{5,\beta}(n,l) \;=\; 0,$$
$$\beta = 1,2,\ldots,N_{\rm rod}, \quad l = 0,1,2,\ldots,N_{5f}-1, \tag{27}$$

where N_{5f} is the number of modes on the faces of rods at $x = x_5$.

We need also the expressions for the amplitudes $A_0^{5,\beta}$ of the waves incident on the plasma. From the continuity conditions of the fields at $x = x_5$ we have

$$A_0^{5,\beta} \;=\; \frac{1}{2} \sum_{n=0}^{N_{\rm tot}-1} \left(\frac{A_n^4}{s_n^4}(1 + \frac{k_0}{k_n^2}) + B_n^4 s_n^4 (1 - \frac{k_0}{k_n^2}) \right) \times$$
$$R^{5,\beta}(n,0), \qquad \beta = 1,2,\ldots,N_{\rm rod}+1. \tag{28}$$

Similarly, for the amplitudes $B_l^{1,\beta}$ of waves reflected back into the waveguides $\{1,1\}$ and $\{1,2\}$, we obtain from the conditions at $x = x_1$

$$2\varepsilon_l B_l^{1,\beta} \;=\; \sum_{n=0}^{N_{\rm tot}-1} \left(A_n^2 s_n^2 (1 - \frac{k_l^1}{k_n^2}) + \frac{B_n^2}{s_n^2}(1 + \frac{k_l^1}{k_n^2}) \right) \times$$
$$R^{1,\beta}(n,l), \quad \beta = 1,2, \quad l = 0,1,2,\ldots,N_1^{\rm prop}. \tag{29}$$

The set of the equations (20), (22), (24-27) has $4N_{\rm tot}$ unknowns and it must hold that $N_{\rm tot} = 2N_{1w} + N_{1f} = (N_{\rm rod}+1)N_{3w} + N_{\rm rod}N_{3f} = (N_{\rm rod}+1)N_{5w} + N_{\rm rod}N_{5f}$. These numbers must be chosen in the agreement with the requirement of the conditioned convergence of the problem of the wave diffraction on the object with edges [22], ie we must try to fulfill the conditions $N_{1w}/N_{1f} = b_1/d_1$, $N_{3w}/N_{3f} = b_3/d_3$ and $N_{5w}/N_{5f} = b_5/d_5$.

The right hand sides of our set are given by the amplitude $A_{l_{\rm inc}}^{1,1}$ of the incident higher mode in the $\{1,1\}$-waveguide and by $N_{\rm rod}+1$ unknown amplitudes $B_0^{5,\beta}$ of the waves reflected from the plasma. To obtain the general solution of our set of linear equations we must solve this system $(N_{\rm rod}+2)$-times setting each time only one from the incident amplitudes equal to 1 and the other to 0. In this way we obtain $N_{\rm rod}+2$ solutions $A_n^2(k)$, $B_n^2(k)$, $A_n^4(k)$, $B_n^4(k)$, $n = 0,1,2,\ldots,N_{\rm tot}$, $k = 1,2,\ldots,N_{\rm rod}+2$. The general solution can be than written as

$$A_n^2 \;=\; A_n^2(1) A_{l_{\rm inc}}^{1,1} + \sum_{\gamma=1}^{N_{\rm rod}+1} A_n^2(\gamma+1) B_0^{5,\gamma}, \quad n = 0,1,2,\ldots,N_{\rm tot}-1. \tag{30}$$

and the similar expressions for B_n^2, A_n^1, B_n^1.

If we insert the general solutions (30) into (28) and rearrange the terms we obtain the explicit expressions for the amplitude transmission and reflection coefficients at $x = x_5$

$$\tau_\beta = \frac{1}{2}\sum_{n=0}^{N_{\rm tot}-1}\left(\frac{A_n^1(1)}{s_n^1}(1+\frac{k_0}{k_n^2}) + B_n^1(1)s_n^1(1-\frac{k_0}{k_n^2})\right) R^{5,\beta}(n,0). \qquad (31)$$

$$\rho_{\beta\gamma} = \frac{1}{2}\sum_{n=0}^{N_{\rm tot}-1}\left(\frac{A_n^1(\gamma+1)}{s_n^1}(1+\frac{k_0}{k_n^2}) + B_n^1(\gamma+1)s_n^1(1-\frac{k_0}{k_n^2})\right) \times$$
$$R^{5,\beta}(n,0), \quad \beta,\gamma = 1,2,\ldots,N_{\rm rod}+1. \qquad (32)$$

Finally, if we insert the general solutions (30) into (29) and rearrange the terms we obtain the explicit expressions for the amplitude transmission and reflection coefficients at $x = x_1$

$$\tau_{1,\beta\gamma}^m = \frac{1}{2\varepsilon_m}\sum_{n=0}^{N_{\rm tot}-1}\left(A_n^2(\gamma+1)s_n^2(1-\frac{k_m^1}{k_n^2}) + \frac{B_n^2(\gamma+1)}{s_n^2}(1+\frac{k_m^1}{k_n^2})\right) \times$$
$$R^{1,\beta}(n,m), \quad m = 0,1,2,\ldots,N_1^{\rm prop}. \qquad (33)$$

$$\rho_{1,\beta}^m = \frac{1}{2\varepsilon_m}\sum_{n=0}^{N_{\rm tot}-1}\left(A_n^2(1)s_n^2(1-\frac{k_m^1}{k_n^2}) + \frac{B_n^2(1)}{s_n^2}(1+\frac{k_m^1}{k_n^2})\right) \times$$
$$R^{1,\beta}(n,m), \quad \beta,\gamma = 1,2,\ldots,N_{\rm rod}+1. \qquad (34)$$

Acknowledgements

The author wishes to thank to M.I. Petelin for the discussion which initiated the work on the problem of the quasi-optical grill mounted in the hyperguide cavity. He acknowledges many constructive remarks from R. Klíma, K. Koláček and F. Žáček. The work was partly supported by the Grants No. 143103 and No. 143405 of Czech Academy of Sciences and partly sponsored by the U.S. - Czech Science and Technology Joint Fund in the cooperation with Czech Ministry of Education and DOE under Project Number 93067.

References

[1] BIBET, P., LITAUDON, X., MOREAU, D., Proc. of IAEA Tech. Committee Meeting on RF Launchers for Plasma Heating and Current Drive, Naka, Japan (1993); see also Lower hybrid heating and current drive in ITER operation scenarios and outline system design, Rep EUR-CEA-FC-1529, Centre d'etude de Cadarache (1994).

[2] PETELIN, M.I., SUVOROV, E.V., Sov. Tech. Phys. Lett. **15** (1989) 882

[3] KOVALEV, N.F., PETELIN, M.I., SUVOROV, E.V., Proc. of the Europhysics topical conference on RF Heating and CD of Fusion Devices, Brussels (1992) 89.

[4] FREZZA, F., SCHETTINI, G., GORI, F., SANTARSIERO, M., SANTINI F., Nucl. Fusion **34** (1994) 1239.

[5] CRENN, J.P., BIBET, P., Quasi-optical grill using diffraction gratings for lower-hybrid waves systems, Rep EUR-CEA-FC-1508, Centre d'etude de Cadarache (1994).

[6] ŽÁČEK, F., KLÍMA, R., PAVLO, P., et al., Design of the quasi-optical grill for lower hybrid current drive on the CASTOR tokamak, Proc. 21st Eur. Conf. on Contr. Fusion and Plasma Physics, Montpellier 1994. Contributed Papers, Vol. 18B, Part III (1994) 1078.

[7] PREINHAELTER, J., Nucl. Fusion **29** (1989) 1729.

[8] ŽÁČEK, F., BADALEC, J., JAKUBKA, K. et al., LHCD experiments on tokamak CASTOR, Proc. of 10th European School on Plasma Physics, Tbilisi 1990, World Scientific, Singapore (1991) 49.

[9] JONES, D.S., The Theory of Electromagnetism, Pergamon Press, Oxford (1964).

[10] BRAMBILLA, M., Nucl. Fusion **16** (1976) 47.

[11] GOLANT, V.E., Zh. Tekh. Fiz. **41** (1971) 2492.

[12] STEVENS, J., ONO, M., HORTON, R., WILSON, J.R., Nucl. Fusion **21** (1981) 1259.

[13] BARANOV, YU.F., SHCHERBININ, O.N., Fiz. plazmy **3** (1977) 246.

[14] LITAUDON, X., BERGER-BY, G., BIBET P. et al., Nucl. Fusion **32** (1992) 1883.

[15] HUŘŤÁK, O., PREINHAELTER, J., IEEE Plasma Science **20** (1992) 425.

[16] HUŘŤÁK, O., Plasma Phys. and Control. Fusion, **32** (1990) 623

[17] PREINHAELTER, J., Czech. J. Phys. B **40** (1990) 527.

[18] PETELIN, M.I., KOVALEV, N.F., SUVOROV, E.V., Quasi-optical diffraction grill for excitation of lower-hybrid waves in tokamaks, Proc. 21st Eur. Conf. on Contr. Fusion and Plasma Physics, Montpellier 1994, Contributed Papers, Vol. 18B, Part III (1994) 1070.

[19] AGARICI, G., BERGER-BY, G., BIBET, P., et al., Quasi-optical lower-hybrid wave launcher experiment in TORE SUPRA, Rep. EUR-CEA-FC-Draft version 1 24.2.95, Centre d'etude de Cadarache (1995).

[20] KAYE, A.S., Progress in ICRH and Lower Hybrid Launcher Development. Plasma Phys. and Control. Fusion **35** (1993) Suppl. A, 71.

[21] MITRA, R., LEE, S.W., Analytical Techniques in the Theory of Guided Waves, MacMillan, New York (1971).

[22] WU, C.P., Computer Techniques for Electromagnetism, Pergamon Press. Oxford (1973).